Monodisperse Droplet Formation Through a Continuous Jet Break-Up Using Glass Nozzles Operated with Piezoelectric Pulsation

Winston Duo Wu, Sean Xuqi Lin, and Xiao Dong Chen
Dept. of Chemical Engineering, Monash University, Clayton Campus, Melbourne, VIC 3800, Australia

DOI 10.1002/aic.12364
Published online July 30, 2010 in Wiley Online Library (wileyonlinelibrary.com).

In this article, a glass nozzle driven by piezoceramics is used to experimentally study the continuous generation of a stream of monodisperse droplets from the breakup of a liquid jet. The approach is demonstrated by examining the breakup dynamics of three distinct liquids. The droplet formation process has been found to be highly controllable and reproducible. The dependence of nozzle performance on liquid properties, flow rate, and disturbance frequency has been investigated. The ratio between the actual disturbance frequency and Reynolds number, ω, is employed at first to represent the operating range that facilitates monodisperse droplet formation. Then, the dimensionless quantity ω^*, obtained by multiplying ω by the viscous characteristic time, $r_j^2/(\mu/\rho)$, has been shown to collapse the data for the lower and higher bounds of the actual disturbance frequency ranges that secure monodispersity of the droplets of all the samples tested. The impacts of liquid flow rate and disturbance frequency on the monodisperse droplet size and spacing between two neighboring droplets have been investigated and discussed.
 AIChE J, 57: 1386–1392, 2011
Keywords: glass nozzles, continuous jet break-up, monodisperse droplet formation, semi-monodisperse droplets, flow rate, disturbance frequency

Introduction

The technology of producing fine and monodisperse droplets was initially developed to improve the resolution of ink-jet printing. Since then it has been expanded to broader fields, such as chemical deposition, DNA arraying, polymer electronics manufacture, production of functional particles and microcapsules, etc. These applications all need to control droplet size and size distribution, and the common goal is often to obtain as uniform, controllable, and reproducible small droplets as possible. For instance, there is typically a desirable particle size to maximize the efficacy of the drug delivery or release kinetics. Micro-fluidic devices are the recent attemps for such purposes and the general introductions to developed micro-fluidic devices for producing uniform droplets can be found elsewhere.[1–5] Most of the current microfluidic devices, however, suffer from a few drawbacks, such as complicated manufacture procedures, poor controllability, poor reproducibility, and limited yield, etc.

Droplet formation is governed by a delicate balance between a number of forces which include gravitational force, inertial force, electric force, mechanical force, aerodynamic force, surface tension force, and viscous force. The net effect of these forces imposed on the liquid make it drip, or form a laminar, wavy or turbulent jet.[6] Monodisperse droplet generation can be obtained by dripping,[7] drop-on-demand type of drop formation,[8,9] and stable disintegration of continuous laminar liquid jet.[10] When studying the continuous break-up of the laminar, non-viscous liquid jet influenced by adequate surface tension, Rayleigh[10] showed

Correspondence concerning this article should be addressed to X. D. Chen at dong.chen@eng.monash.edu.au.

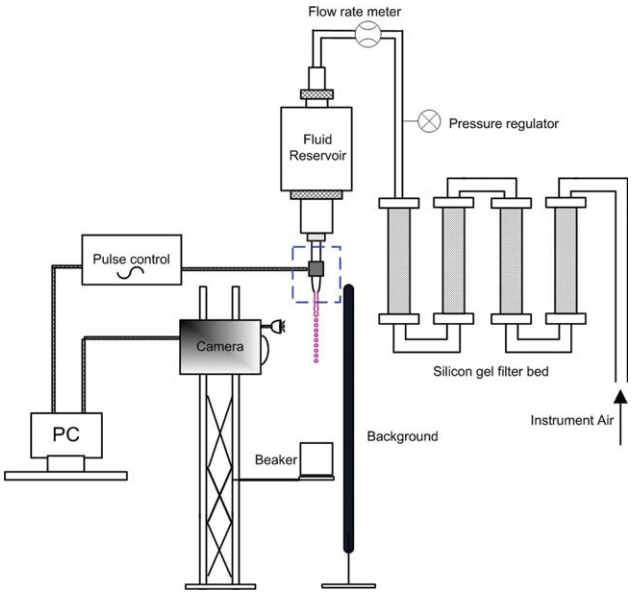

Figure 1. Schematic graph of the experimental set-up.

[Color figure can be viewed in the online issue, which is available at wileyonlinelibrary.com.]

mathematically that all disturbances on the jet with wavelengths greater than λ_{min} ($\lambda_{min} = 2\ \pi r_j$) would propagate down the jet and grow in amplitude, and deduced analytically that the disturbance with the optimum wavelength $\lambda_{opt} = 9.02\ r_j$ had the fastest growth rate and the spacing (S_0) between two neighboring droplets equal to the disturbance wavelength when monodisperse droplets were obtained (r_j is the radius of liquid jet). In other words, λ_{opt} guarantees droplet monodispersity. In addition, the volume of the monodisperse droplet formed with the radius (r_0) must be equal to the volume of the liquid column of the length λ_{opt}, i.e.,

$$\lambda_{opt}\pi r_j^2 = \frac{4}{3}\pi r_0^3 \tag{1}$$

To take the viscosity of the liquid jet into account, Weber[11] extended the Rayleigh theory to be more general for laminar jet break-up. The optimum disturbance wavelength (λ_{opt}) based on a consideration of surface energy to break up the jet into droplets was described as:

$$\lambda_{opt} = \sqrt{8}\pi r_j\left(1 + \frac{3\mu}{\sqrt{2\rho\sigma r_j}}\right) \tag{2}$$

where ρ is the density of the liquid (kg m^{-3}), σ is the surface tension of the liquid (N m^{-1}), and μ is the viscosity of the liquid (Pa s).

In fact, besides the optimum wavelength, there is normally a range of disturbance wavelength (λ_{dis}) that can facilitate monodisperse droplet formation for a certain liquid. This was found in this sudy and shown in Figure 3. The disturbance wavelength is equal to the ratio of the velocity of the liquid jet (v_j, m s^{-1}) to the disturbance frequency (f_{dis}) as:

$$\lambda_{dis} = \frac{v_j}{f_{dis}} \tag{3}$$

In this work, we report experiment results on a specially designed piezoelectric glass nozzle to produce monodisperse droplets and to present the investigations on the relationships of droplet size, liquid properties (density, viscosity, and surface tension), flow rate, and disturbance frequency.

Experimental

The schematic graph of the experimental set-up is shown in Figure 1. The reservoir was filled with pre-filtered liquid

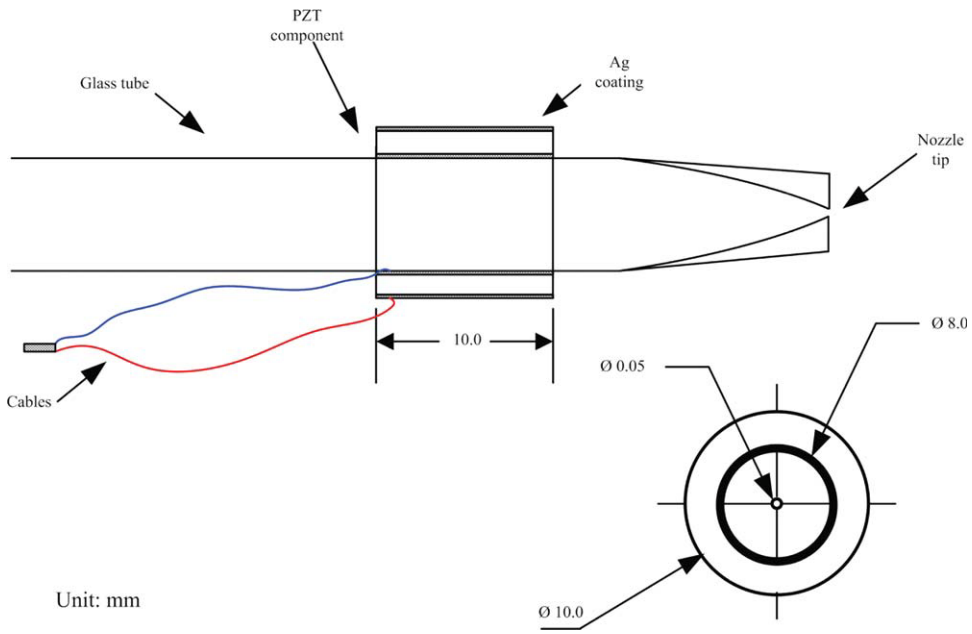

Figure 2. Schematic graph of the specially designed nozzle structure.

[Color figure can be viewed in the online issue, which is available at wileyonlinelibrary.com.]

Table 1. The Compositions and Properties of Three Testing Samples

Sample Number (#)	Composition			Property		
	Na-alginate (Wt %)	Vitamin B12 (Wt %)	Lactose (Wt %)	Viscosity (Kg m^{-1} s^{-1})	Surface Tension (Nm^{-1})	Density (Kg m^{-3})
1	0.5	0.05	5	0.0402	0.6846	979.3
2	0.7	0.07	5	0.0544	0.6561	989.8
3	0.9	0.09	5	0.0948	0.6452	1010.3

(to avoid blockage of the nozzle) to be jetted using the nozzle system. Dehumidified instrument air was used to force the liquid to jet from the orifice. The "specially designed" nozzle was manufactured by surrounding a glass capillary with a piezoelectric ceramic component (APC international).[12] Figure 2 shows the schematic structure of the nozzle. The orifice radius of the capillary utilized here is 60 μm. By adjusting the back pressure of the reservoir, it was possible to control the velocity of the liquid jet. The jet was broken down by transferring a sinusoidal electrical signal of frequency (f_{set}) from a pulse generator (Microfab Technologies) to the piezoelectric component to regularly squeeze the glass capillary. The velocity of the liquid jet was calculated as $v_j = v_m/\rho\pi r_j^2$, where v_m is the mass flow rate ($kg{\cdot}s^{-1}$) which was experimentally measured. To investigate the droplet formation process (i.e., jet diameter, droplet spacing, size, and size distribution), photographs were taken using a digital SLR camera (Nikon, D40×) with a strobe (Nikon SB-400) and a micro-lens (AF Micro-Nikkor 60 mm f/2.8D). A ruler was placed in each shot beside the liquid stream to serve as an indicator for benchmarking the distance the droplets had travelled away from the nozzle orifice. Three test samples were composed with pharmaceutical materials as various amounts of Na-alginate, Vitamin B12, and monohydrate Alpha-*D*-lactose powders [Sigma (Australia)] dissolved in distilled water. Accordingly, the solutions had different liquid properties, as listed in Table 1. The viscosity was found to increase significantly at higher concentrations of Na-alginate, while the surface tension and density had little difference for these three test samples.

The formation mechanism of monodisperse droplets is influenced by liquid properties, liquid flow rate, and actual disturbance frequency. The flow rate controlled by applying different pressures to the liquid reservoir must meet the jet velocity requirement to ensure the laminar flow. Within the velocity range that Sakai and Hoshino[13] proposed to realize laminar flow, three different flow rates were selected for each testing liquid. The desirable disturbance frequencies were found by tuning the set-up frequency of the sinusoidal electrical signal from 1 to 40 kHz. A series of photographs of jet break-up of the #2 sample in different disturbance frequencies and at the constant mass flow rate of 1.3 g min^{-1} are shown in Figure 3. The droplet formation process was precisely monitored. From the images, the range of the set-up disturbance frequencies that facilitated monodisperse droplet formation had been identified. Furthermore, the spacing between neighboring droplets and droplet size was measured with the relative error smaller than 2%, averaged among three repeated measurements, and analyzed through the image processing and analysis software, ImageJ™.

Results and Discussion

As shown in Figure 3, when the disturbance frequency is low (such as below 3 kHz), the liquid jet breaking-up process is irregular. The liquid jet breaks into droplets more

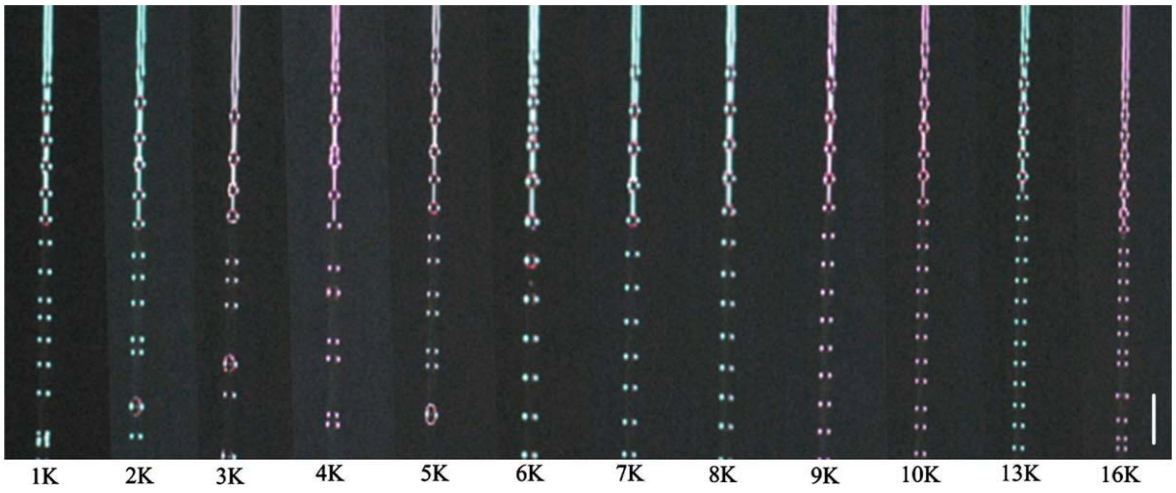

Figure 3. A series of photographs of the droplet formation processes of #2 sample in varied disturbance frequencies (kHz) within the constant mass flow rate of 1.3 g min^{-1}. Scale bar: 1 mm.

[Color figure can be viewed in the online issue, which is available at wileyonlinelibrary.com.]

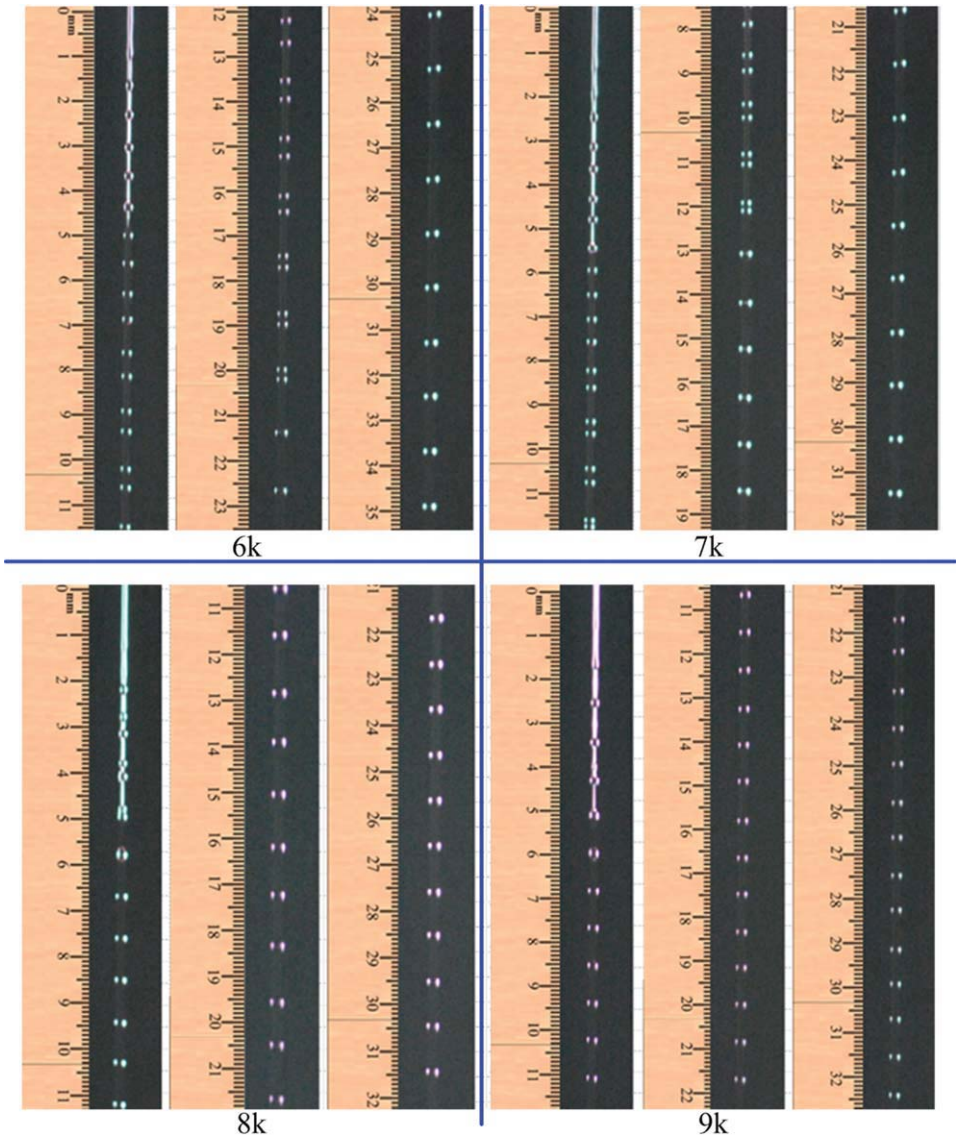

Figure 4. The photographs of the droplet formation and traveling process of #1 sample in varied disturbance frequencies (kHz) at the constant mass flow rate of 1.69 g min^{-1}.

[Color figure can be viewed in the online issue, which is available at wileyonlinelibrary.com.]

regularly at larger disturbance frequencies. However, if it is too high (for example, above 16 kHz), the break-up process becomes irregular again. It can be shown that monodisperse droplets are produced among the medium range of disturbance frequencies. Interestingly, there are disturbance frequencies at which droplets are initially monodisperse, and then they recoil together in pairs after traveling for a few millimeters. The phenomenon may be called as ''semi-monodisperse droplet formation.'' The qualitative difference between monodisperse and semi-monodisperse droplet formation is illuminated in Figure 4, which shows the sequential photographs of the droplet regime of #1 sample at the constant mass flow rate of 1.69 g min^{-1} and at, respectively, the disturbance frequencies of 6, 7, 8, and 9 kHz. The disturbance frequencies of 6 kHz and 7 kHz produced the ''semi-monodisperse'' droplet formation where every couple of initially monodisperse, but smaller droplets get closer and closer to each other as they travel down, and finally coalesce into uniform but bigger droplets after traveling for 21.5 mm and 13.1 mm, respectively, below the orifice. This phenomenon might be viewed as follows: the upper droplet in the couple of coalescing droplets consistently breaks first at its upstream end, and after breaking up with the lower droplet, the forces acting between this couple of droplets make the traveling velocity of upper droplet larger than that of lower droplet until they rejoin. Genuine monodisperse droplets were seen to form at the disturbance frequencies of 8 kHz and 9 kHz. The droplets were formed one by one, and the spacing between neighboring droplets was uniform and equal to the actual disturbance wavelength. By considering the influence

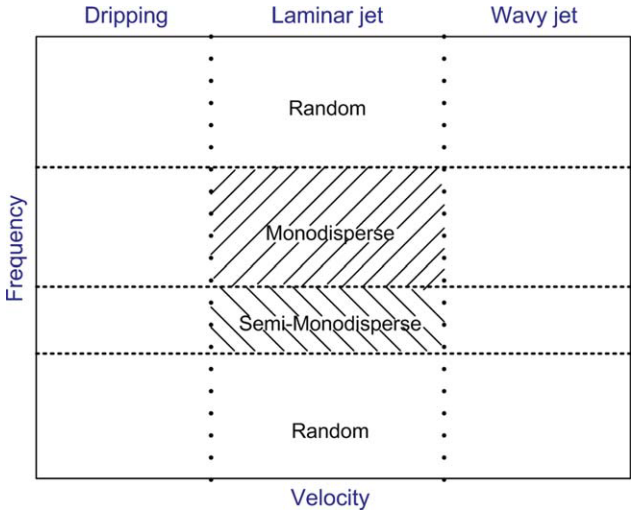

Figure 5. The qualitative map of droplet formation process with different conditions of flow rate and disturbance frequency.

[Color figure can be viewed in the online issue, which is available at wileyonlinelibrary.com.]

of the jet velocity and disturbance frequency, the conditions that produced random, semi-monodisperse, and monodisperse droplets are qualitatively shown in the Figure 5.

To investigate the quantitative relationship between the flow rate and the disturbance frequency, the dimensionless wave number (k) is introduced:

$$k = \frac{2\pi r_j}{\lambda_{act}} = \frac{2\pi r_j f_{act}}{v_j} \tag{4}$$

where λ_{act} and f_{act} are the actual disturbance wavelength and frequency, respectively. f_{act} can be calculated by:

$$f_{act} = \frac{v_m}{\rho \frac{4}{3}\pi r_0^3} \tag{5}$$

From operability point of view, it is desirable to predict, or at least correlate, the corresponding range of disturbance frequency to a given jet velocity which can facilitate monodisperse droplet formation. Sakai and Hoshino[13] and Wildeboer et al.[14] proposed that the stability region for mono-sized droplet formation (Figures 2 and 4 in Ref. 14) could be recognized based on the ratio between f_{act} and v_j. It is interesting to note that this (previous) analysis seems to have not taken into account the direct proportionality (according to Eq. 4) between the disturbance frequency and flow velocity.

It is noted that the relationship between the actual disturbance frequency (f_{act}) and the set frequency for the piezoelectric material (f_{set}), is straightforward (see Appendix) and seems not affected much by the sample properties.

In this study, to consider the effect of liquid properties (i.e., viscosity), disturbance frequency, and flow rate on monodisperse droplet production, the plot of f_{act} against Re (Re is the Reynolds number which is defined as $\rho v r_j/\mu$) was found to yield a clear trend which is useful as an operability guidance, as shown in Figure 6. The ratio between actual disturbance frequency and Reynolds number, denoted as ω, has a particular range for monodisperse droplet formation.

$$\omega = \frac{f_{act}}{\mathrm{Re}} = \frac{k\mu}{4\rho\pi r_j^2} \tag{6}$$

Three different flow rates, corresponding to three values of Re were applied to each of the three samples. The set-up disturbance frequency was tuned to find the lower bound and the higher bound that can realize monodisperse droplet formation. For example as shown in Figure 6, under three different Re: 3.96, 4.99, and 7.18, the minimum f_{act} values to produce monodisperse droplets for sample #2 are 1.43, 1.77, and 2.6 kHz, respectively, while the maximum f_{act} values are 3.68, 4.49, and 6.1 kHz, respectively. The values of ω for the lower and higher bounds are roughly constant at 0.36 and 0.9, respectively. Based on this finding, in a rectangular coordinate with Re and f_{act} as abscissa and ordinate, respectively, two straight lines from the origin with the slope equal to the lower and higher bounds of ω, respectively, can be worked out to contain the region of monodispersity. Given Re for a certain liquid, the range of f_{act} to produce uniform droplets can then be identified. Similar trend has been found for the other two liquid samples. With increasing viscosity, the value of ω becomes larger while the range between the lower and higher bounds becomes wider.

To generalize the above discussion to broader range of fluids, ω can be normalized. Here, the characteristic viscous time, $r_j^2/(\mu/\rho)$ was multiplied to ω, giving:

$$\omega* = \omega\frac{r_j^2}{\mu/\rho} = \frac{f_{act}}{v_j/r_j} \tag{7}$$

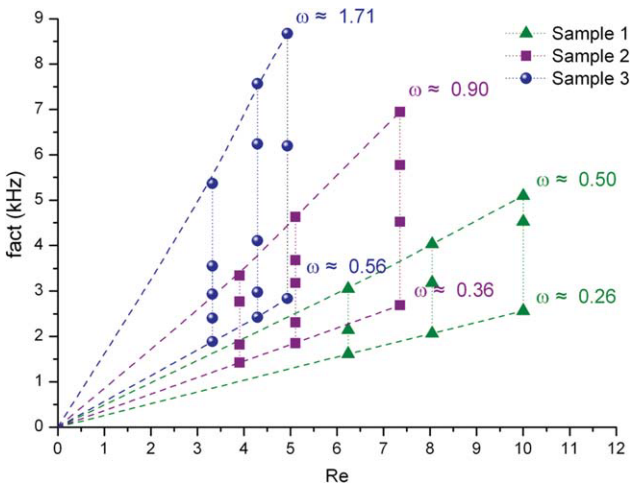

Figure 6. The experiment results for the range of the ratio (ω) between actual disturbance frequency (f_{act}) and Reynolds number (Re) to facilitate monodisperse droplet formation for three different liquid samples.

[Color figure can be viewed in the online issue, which is available at wileyonlinelibrary.com.]

For individual samples, every tested liquid velocity had the corresponding lowest and highest actual disturbance frequencies which can facilitate monodisperse droplet formation. The lower bound (ω^*_{low}) and the higher bound (ω^*_{high}) of ω^*, for instance for #1 sample at three different velocities of 1.47, 1.89, and 2.36 m s^{-1}, was 0.55 and 1.04, 0.55 and 1.06, 0.54 and 1.08, respectively. Interestingly, ω^*_{low} and ω^*_{high} for all the three different samples averaged at various velocities was found to be similar at ~0.47 and ~1.12, respectively, as shown in Figure 7.

Over the range of the disturbance frequencies that allow monodisperse droplet formation, the droplet size and the spacing between neighboring droplets (equivalent to the actual disturbance wavelength) were calculated (using Eq. 5) and measured. Figure 8 illustrates the results of such calculation and measurement for each of the liquid samples at *Re* of 4.5. For individual liquid samples, the monodisperse droplet size was reduced with increasing set-up disturbance frequency, and the estimated droplet size according to the theoretical formula (i.e., Eq. 1) was slightly smaller than the measured droplet size. This might be due to size measurement errors resulted from blurred edges of photographed droplets. At *Re* of 4.5, larger disturbance frequency was required for the more viscous liquid sample to produce monodisperse droplets. In addition, the range of appropriate disturbance frequencies for the more viscous liquid samples was wider, and there were some overlaps between the ranges for each sample, which was in good agreement with the results illustrated by Figure 6. With the same disturbance frequency, the monodisperse droplet size was larger for the more viscous liquid.

Conclusions

We have demonstrated that monodisperse droplets can be produced by the piezoceramics-driven glass nozzles that are specially constructed for this study. Three liquid samples with different fluid properties were tested. The droplet formation process was monitored by the SLR digital camera with the micro-lens and strobe, such that the ranges of disturbance frequency that facilitate monodisperse droplet formation are identified. A new regime called as "semi-monodisperse droplet formation" has been identified. The qualitative trend of varying disturbance frequency to obtain random, semi-monodisperse, monodisperse droplets has been demonstrated. In the case of producing monodisperse droplets, from the operability point of view, the ratio between the actual disturbance frequency and Reynolds number, ω, has been shown to represent the high and low limits of the range of disturbance frequency that facilitates monodisperse droplet formation. Moreover, ω was normalized (ω^*) by multiplying it with the characteristic viscous time, $r_j^2/(\mu/\rho)$. The normalized ω^* has been seen to have unique lower bound and higher bound values. For a particular liquid, the monodisperse droplet size can be reduced by increasing the disturbance frequency. The more viscous liquid has a wider range of disturbance frequencies that can produce monodisperse droplets while leading to larger monodisperse droplets at the same Reynolds number and disturbance frequency. The formation process has been seen to be highly controllable and reproducible. The full theoretical analysis of the dependence of the liquid jet break-up on liquid properties is beyond the scope of this study, and some have been treated elsewhere.[15,16] Though the nozzle was specially designed for this study, the trends observed in this work may well be applicable to other types of nozzles generated through piezoelectric technology with similar working mechanism, such as commercially available nozzles manufactured by Microfab in USA and Microdrop in Germany.[1] Since the trends are well recognized, this specially designed nozzle with different orifice sizes are expected to find applications in wider field.

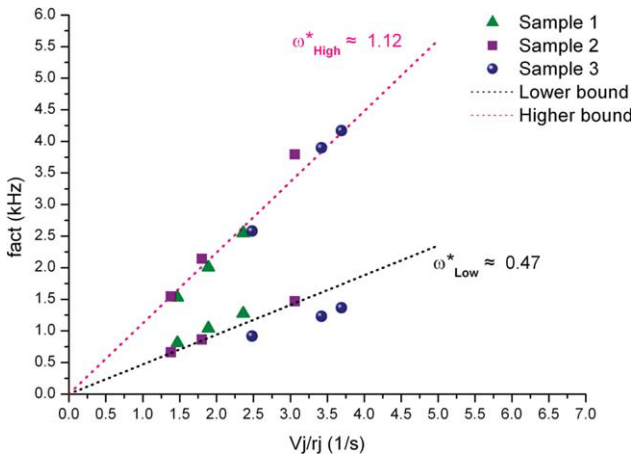

Figure 7. The dimensionless representation of the general operability region for monodisperse droplet formation.

[Color figure can be viewed in the online issue, which is available at wileyonlinelibrary.com.]

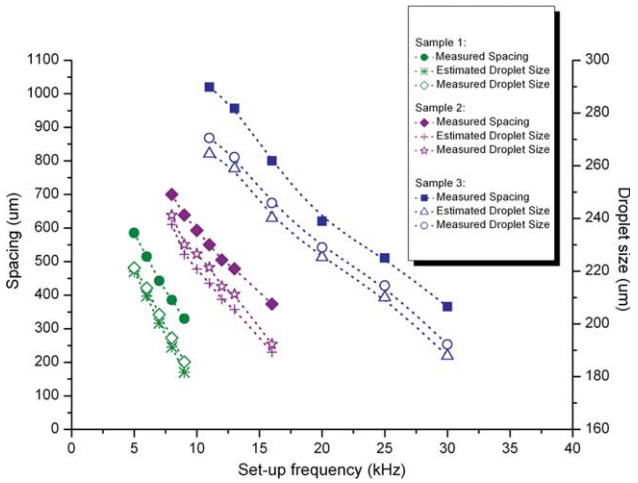

Figure 8. The calculated droplet size and measured spacing between neighboring droplets and droplet size under respective disturbance frequency range producing monodisperse droplets for each of liquid sample under the same *Re* of 4.5.

[Color figure can be viewed in the online issue, which is available at wileyonlinelibrary.com.]

Acknowledgments

The authors thank Mr. Samuel Rogers and Dr. Kamlesh Patel for helpful discussions. This work has been supported by ARC Discovery Grant DP0773688.

Notation

f_{act} = actual disturbance wavelength ($1 \cdot s^{-1}$)
f_{dis} = disturbance frequency ($1 \cdot s^{-1}$)
k = wave number
Oh = Ohnesorge number
Re = Reynolds number
r_j = liquid jet radius (m)
r_c = circular orifice size (m)
r_0 = droplet radius (m)
S_0 = droplet spacing (m)
v_j = liquid jet velocity (m s^{-1})
v_m = liquid jet mass flow rate (kg s^{-1})

Greek letters

λ_{min} = minimum disturbance wavelength (m)
λ_{opt} = optical disturbance wavelength (m)
μ = viscosity of the liquid (Pa s)
ρ = density of the liquid (kg m^{-3})
σ = surface tension coefficient of the liquid (N m^{-1})
ω = ratio between actual disturbance frequency and Reynolds number

Literature Cited

1. Basaran OA. Small-scale free surface flows with breakup: drop formation and emerging applications. *AIChE J*. 2002;48:1842–1848.
2. Kobayashi I, Nakajima M. Silicon array of elongated through-holes for monodisperse emulsion droplets. *AIChE J*. 2002;48:1639–1644.
3. Wu DW, Patel K, Rogers S, Chen XD. Monodisperse droplet generators as potential atomizers for spray drying technology. *Dry Technol*. 2007;25:1907–1916.
4. Yamamoto T, Endo A, Eiad-ua A, Ohmori T, Nakaiwa M, Soottitantawat A. Synthesis of monodisperse carbon beads with developed mesoporosity. *AIChE J*. 2007;53:746–749.
5. Xu JH, Li SW, Tan J, Wang YJ, Luo GS. Preparation of highly monodisperse droplet in a T-Junction microfluidic device. *AIChE J*. 2006;52:3005–3010.
6. Clift R, Grace JR, Weber ME. *Bubbles, Drops, and Particles*. London: Academic Press, 1978.
7. Ambravaneswaran B, Subramani HJ, Phillips SD, Basaran OA. Dripping-jetting transitions in a dripping faucet. *Phys Rev Lett*. 2004; 93:034501–034504.
8. Chen AU, Basaran OA. A new method for significantly reducing drop radius without reducing nozzle radius in drop-on-demand drop production. *Phys Fluids*. 2002;14:L1–L4.
9. Dong HM, Carr WW. An experimental study of drop-on-demand drop. *Phys Fluids*. 2006;18:072102-1–072102-16.
10. Rayleigh L. On the stability of jets. *P Lond Math Soc*. 1878;10: 4–13.
11. Weber C. Zum zerfall eines flussighkeitesstrahles. *Z Angew Math Mech*. 1931;11:136–154.
12. Lee ER. *Microdrop Generation*. Boca Raton, FL: CRC Press, 2002.
13. Sakai T, Hoshino N. Production of uniform droplets by longitudinal vibration of audio frequency. *J Chem Eng Jpn*. 1980;13:263–268.
14. Wildeboer WJ, Koppendraaier E, Litster JD, Howes T, Meesters G. A novel nucleation apparatus for regime separated granulation. *Powder Technol*. 2007;171:96–105.
15. Gañán-Calvo AM. Generation of steady liquid microthreads and micron-sized monodisperse sprays in gas streams. *Phys Rev Lett*. 1998;80:285–288.
16. Eggers J. Nonlinear dynamics and breakup of free-surface flows. *Rev Mod Phys*. 1997;69:865–930.

Appendix

For the three test fluids used in the current study and for the mono-disperse droplet generation at three different velocity levels (refer to Figure 6), respectively, the data points of f_{act} and f_{set} are plotted in Figure A1. There appears to be no obvious dependency on the types of fluids and the velocities in the range tested hence a unique correlation is established:

$$f_{act} = 7.238741 \times 10^2 \cdot \exp(1.229121 \times 10^{-4} \cdot f_{set}) \quad \text{(A1)}$$

The correlation coefficient r^2 is 0.8538.

Although this correlation may be nozzle type dependent, it serves the purpose to show the general trend. In future, detailed mechanistic analysis of the system may be benchmarked against the trend illustrated here.

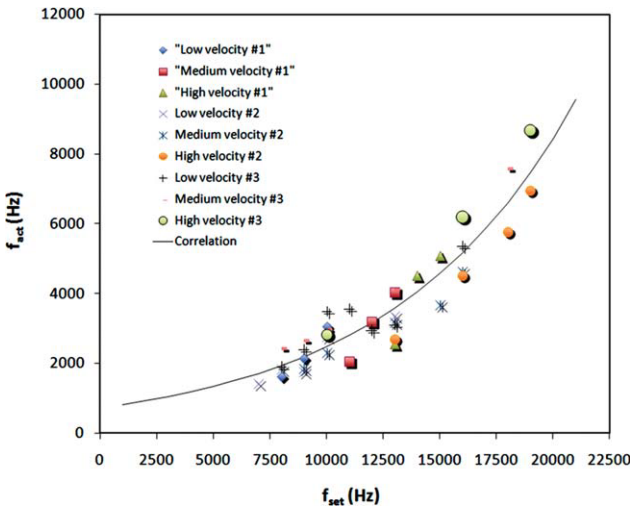

Figure A1. Relationship between the actual disturbance frequency and the set frequency of the piezoelectric material.

[Color figure can be viewed in the online issue, which is available at wileyonlinelibrary.com.]

Manuscript received Jan. 23, 2009, revision received May 7, 2010, and final revision received Jun. 30, 2010.